Sensitivity Measures for Minimizing Model Uncertainty in Probabilistic Analysis

M. Mahsuli[1] and T. Haukaas[2]
[1] *PhD Candidate, Department of Civil Engineering, University of British Columbia, Vancouver, Canada, mahsuli@gmail.com*
[2] *Associate Professor, Department of Civil Engineering, University of British Columbia, Vancouver, Canada, terje@civil.ubc.ca*

Abstract: This paper presents a new set of reliability sensitivity measures. The purpose with these measures is to identify the optimal manner in which to reduce model uncertainty in order to improve risk estimates. In particular, two sensitivity measures are presented. One identifies the buildings, or other components within a region, that should be subjected to more refined modeling. The other sensitivity measure identifies model types that should be subjected to further research to improve the model form. The developments in this paper are presented in the context of a region with 622 buildings that are subjected to seismic hazard. A comprehensive seismic risk analysis is conducted with approximately 300 random variables, more than 30 different model types, and more than 3,000 individual model instances. All models are probabilistic and emphasis is placed on explicit characterization of epistemic uncertainty, *i.e.*, reducible uncertainty. The models are available in a new computer program called Rt, which is tailored for reliability analysis with multiple probabilistic models. The primary result from the analysis is risk estimates, presented in the form of loss probability curves. However, focus in this paper is on the development and evaluation of sensitivity measures, in order to guide efforts to reduce the model uncertainty and thus improve the risk estimates. For the considered region it is found that concrete shear wall buildings, and structural response models for such buildings, rank highest according to both sensitivity measures. As described in this paper, this means that allocating resources for detailed analysis and improved models for this type of building has the greatest impact on the risk estimates.

Keywords: Probabilistic models, model uncertainty, sensitivity analysis, risk, reliability

1. Introduction

The primary objective in this paper is to identify the optimal course of action to reduce model uncertainty. Context is provided by seismic risk analysis, where multiple probabilistic models are employed for hazard, infrastructure, and impacts. In this paper, reliability methods are utilized in conjunction with a library of probabilistic models to make predictions about potential future seismic losses. The analysis is carried out with a new reliability-based risk analysis program, called Rt, which is specifically developed for multi-model reliability and optimization analysis. Rt is freely available online at www.inrisk.ubc.ca. The library of probabilistic models is implemented in Rt, and certain models are devoted particular attention in this paper. However, although the study is focused on seismic risk, the methods and models are generic. In fact, the developments in this paper are intended as universal techniques for the recognition and subsequent reduction of epistemic uncertainty, *i.e.*, reducible uncertainty. To this end, two questions are asked and

5th International Conference on Reliable Engineering Computing (REC 2012)
Edited by M. Vořechovský, V. Sadílek, S. Seitl, V. Veselý, R. L. Muhanna and R. L. Mullen

ISBN 978-80-214-4507-9. Published by Ing. Vladislav Pokorný − LITERA

addressed in this study: 1) Which infrastructure components should be subjected to more detailed modeling to reduce the epistemic uncertainty, in order to improve the quality of the present risk analysis? 2) Which models in the library of probabilistic models should be prioritized in research efforts to reduce the epistemic uncertainty to improve the quality of future risk analyses? The vehicle for the developments is reliability analysis with the limit-state function

$$g = g(\boldsymbol{\theta}, \mathbf{x}, \mathbf{v}) = l_0 - l(\boldsymbol{\theta}, \mathbf{x}, \mathbf{v}) \tag{1}$$

where l_t = loss threshold, $l(\boldsymbol{\theta},\mathbf{x},\mathbf{v})$ = loss due to earthquake damage, $\boldsymbol{\theta}$ = vector of epistemic random variables, $\mathbf{x}$ = vector of aleatory random variables, and $\mathbf{v}$ = vector of decision variables that are at the discretion of the decision maker. The focus in this paper is on the uncertainty described by $\boldsymbol{\theta}$, while the $\mathbf{v}$ is omitted in the following. Reliability methods, such as the first-order and second-order reliability methods and importance sampling, estimates the probability that $g < 0$. As a result, reliability analysis with Eq. (1) yields the probability that the cost l exceeds l_o. In other words, the result is a point on the loss exceedance probability curve, hereafter called loss curve. Loss curve results are presented later in this paper and they appear prominently in several areas of seismic risk analysis. They are particularly popular in the insurance industry and in modern performance-based earthquake engineering.

It is emphasized in this paper that many interacting probabilistic models are required to evaluate $l(\boldsymbol{\theta},\mathbf{x},\mathbf{v})$ in Eq. (1). In fact, a significant effort is made to develop or improve models for all facets of the hazards, infrastructure, and impacts associated with seismic risk. In turn, the models are implemented in Rt to facilitate the communication between the models at run-time. The new object-oriented software architecture to accomplish this is described by Mahsuli and Haukaas (2012). From a broader perspective, Rt is intended as a continuously growing framework of predictive probabilistic models, with explicit characterization of epistemic uncertainty. This is intended to promote targeted future efforts to reduce that uncertainty. In fact, the framework provides a rational basis for allocating resources to gather data and build better models, which ultimately yields improved risk mitigation decisions. This motivates the developments in this paper.

2. Models

The approach adopted in this paper has two components: probabilistic models and reliability methods. In contrast with many contemporary seismic risk analysis approaches, the present approach circumvents conditional probability models in favour of simulation-type models that produce scalars or vectors of physical responses. This is necessary in order to evaluate Eq. (1). In particular, the models that are utilized in this study employ random variables to discretize the uncertainty. A simple but instructive model is the linear regression model

$$y = \theta_1 + \theta_2 \cdot h_2(\mathbf{x}) + \theta_3 \cdot h_3(\mathbf{x}) + \cdots + \varepsilon \tag{2}$$

where y = model response, θ_i = model parameters, $h_i(\mathbf{x})$ = explanatory functions, and ε = zero-mean normally distributed model error. In the Bayesian approach to linear regression for this model, the parameters θ_i and the standard deviation of ε are random variables. This approach is adopted here, where the model parameters are categorized as epistemic random variables, *i.e.*, $\boldsymbol{\theta} = \{\theta_1, \theta_2, \ldots, \sigma_\varepsilon\}$. Furthermore, their probability distribution is affected by model improvement, typically by data gathering efforts. The statistical inference for the random variables in $\boldsymbol{\theta}$ is carried out in accordance with Box and Tiao (1992), Gardoni *et al.* (2002), and others. In fact, the Bayesian modeling philosophy is adopted throughout this study, although the model forms may vary.

In Rt's framework of models, each input variable in $\mathbf{x}$ to Eq. (2) is either provided as a random variable by the analyst or as a response from an "upstream" model. In turn, the response, y, may serve as input to a "downstream" model. For example, one variable in $\mathbf{x}$ may be an earthquake magnitude predicted by another model, while y may be a site-specific ground shaking intensity that serves as input to a building response model.

The specific set of models considered in this paper simulate the occurrence of hazards, building responses, damage, and cost for 622 buildings on the campus of the University of British Columbia (UBC) in Vancouver, Canada. Figure 1 displays a map of the region with the UBC campus identified in reference to downtown Vancouver. The dots in the zoomed map of the UBC campus identify the 622 building on campus. The second author's research group surveyed each building to gather data about building type, building height, footprint area, *etc*.

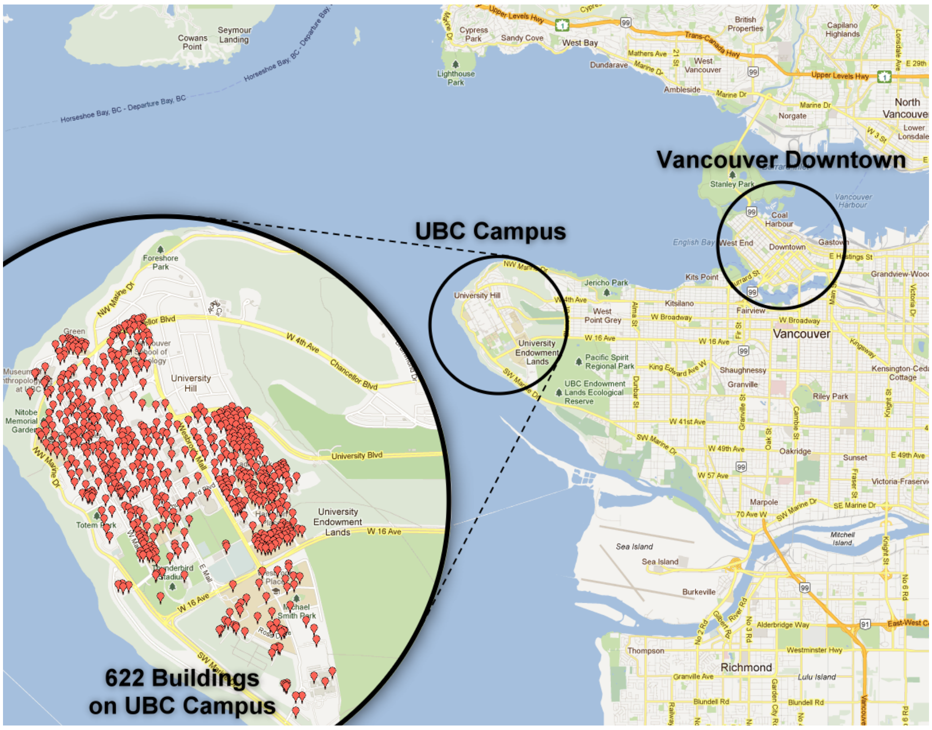

Figure 1. Map of the UBC campus and the 622 buildings that are modeled in this study.

Table I displays some of the information that was gathered for each of the 622 buildings at the UBC campus. For brevity, only some of the buildings are presented. These particular buildings were selected for this table because they appear prominently in the rankings that are presented later in this paper.

Table I: Information for a few selected buildings among the 622 buildings on the UBC campus.

Building Name	Footprint Area (m^2)	Number of Stories	Year Erected	Mean Total Value ($)	Code Level	Longitude	Latitude
Animal Science Main Sheep Unit	552	1	1976	671,109	Moderate	-123.2341	49.2509
Chan Centre for Performing Arts	3,315	1	1997	7,107,360	Moderate	-123.2551	49.2698
Morris & Helen Belkin Art Gallery	1,105	2	1995	4,738,240	Moderate	-123.2562	49.2682
Power House Meter Station	90	1	1960	206,730	Low	-123.2545	49.265
St. Mark Chapel	524	2	1997	2,406,909	Moderate	-123.249	49.2722
University Centre Addition	230	1	1987	528,310	Moderate	-123.2568	49.2691
Vanier Pump Station	16	1	1986	37,277	Moderate	-123.2603	49.2648
Village Shops 1	922	2	1980	4,234,872	Moderate	-123.2428	49.2666
Village Shops 2	1,171	1	1980	2,689,424	Moderate	-123.2434	49.2664
Wesbrook Animal Care Unit	596	1	1981	1,369,012	Moderate	-123.2489	49.2652
…	…	…	…	…	…	…	…

The UBC campus is subjected to three sources of seismicity: Shallow crustal earthquakes, deep subcrustal earthquakes, and megathrust subduction earthquakes. The first two occur within area sources, while subduction earthquakes originate from a faultline that runs under the ocean outside the coastline of the Pacific Northwest.

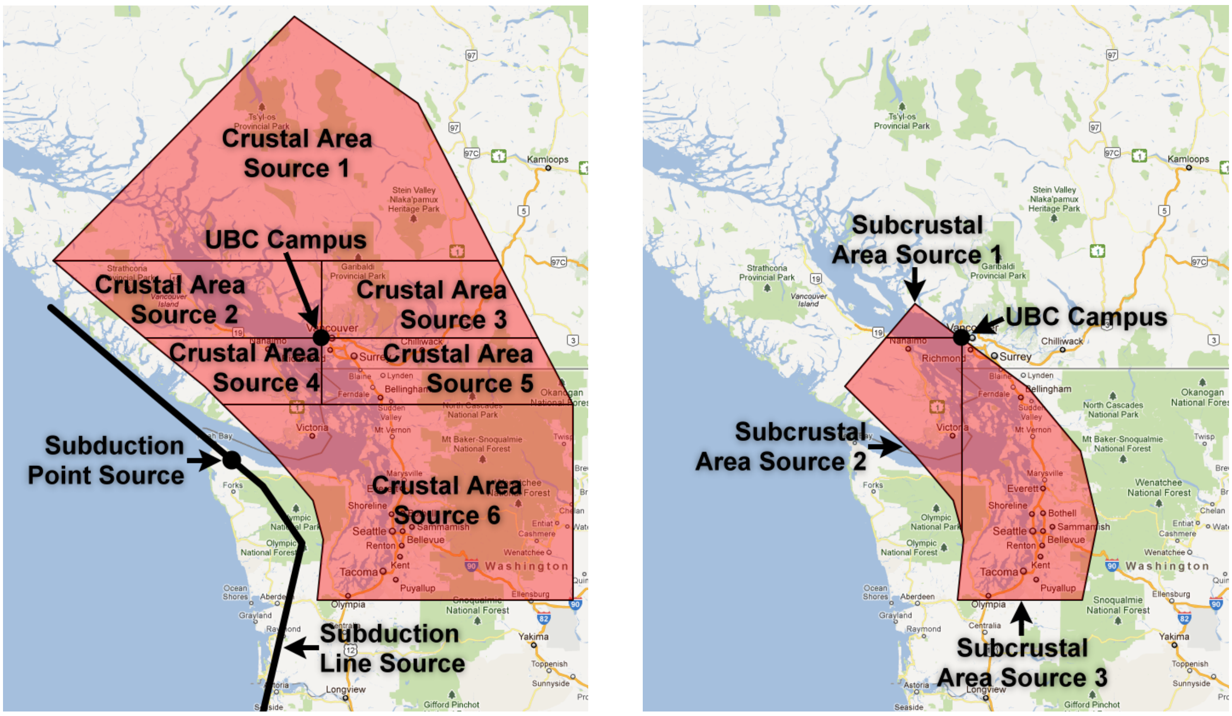

Figure 2. Sources of earthquakes affecting the UBC campus.

Table II: Overview of models employed in the analysis.

Model Name	Formulation	Instances	Size($\mathbf{x}$)	K = Size($\boldsymbol{\theta}$)
Concrete Frame with Masonry Infill Wall Structural Damage	Nonlinear Regression	10	7	9
Concrete Frame with Masonry Infill Wall Structural Response	Linear Regression	10	4	25
Concrete Moment Frame Structural Damage	Nonlinear Regression	22	8	10
Concrete Moment Frame Structural Response	Linear Regression	22	4	25
Concrete Shear Wall Structural Damage	Nonlinear Regression	134	7	9
Concrete Shear Wall Structural Response	Linear Regression	134	4	25
Crustal Intensity	Algorithm	1	4	1
Non-Structural Acceleration Damage	Nonlinear Regression	622	2	3
Non-Structural Drift Damage	Nonlinear Regression	622	2	3
Precast Concrete Structural Damage	Nonlinear Regression	11	8	10
Precast Concrete Structural Response	Linear Regression	11	4	25
Reinforced Masonry Structural Damage	Nonlinear Regression	58	8	10
Reinforced Masonry Structural Response	Linear Regression	58	4	25
Steel Braced Frame Structural Damage	Nonlinear Regression	5	7	9
Steel Braced Frame Structural Response	Linear Regression	5	4	25
Steel Frame with Concrete Shear Wall Structural Damage	Nonlinear Regression	6	6	8
Steel Frame with Concrete Shear Wall Structural Response	Linear Regression	6	4	25
Steel Frame with Masonry Infill Wall Structural Damage	Nonlinear Regression	2	6	8
Steel Frame with Masonry Infill Wall Structural Response	Linear Regression	2	4	25
Steel Light Frame Structural Damage	Nonlinear Regression	22	6	8
Steel Light Frame Structural Response	Linear Regression	22	4	25
Steel Moment Frame Structural Damage	Nonlinear Regression	4	7	9
Steel Moment Frame Structural Response	Linear Regression	4	4	25
Subcrustal Intensity	Algorithm	1	4	1
Subduction Intensity	Algorithm	1	4	1
Unreinforced Masonry Structural Damage	Nonlinear Regression	14	6	8
Unreinforced Masonry Structural Response	Linear Regression	14	4	25
Wood Large Frame Structural Damage	Nonlinear Regression	128	5	7
Wood Large Frame Structural Response	Linear Regression	128	4	25
Wood Light Frame Structural Damage	Nonlinear Regression	206	5	7
Wood Light Frame Structural Response	Linear Regression	206	4	25

It is noted that Figure 2 divides the area sources into several sub-areas. Specifically, the crustal earthquake source is divided into six area sources, while the subcrustal area source is divided into three area sources. This is done for practical reasons that relate to the reliability analysis. In particular, the first-order reliability method (FORM) is employed, and this type of analysis requires a continuously differentiable limit-state function that is relatively linear in the space of the random variables. This is achieved by the subdivision of the area sources in Figure 2. Furthermore, the subduction source is divided into a point source and a line source. This is done for physical reasons. Specifically, a certain range of magnitudes of subduction earthquakes is associated with rupture of the entire fault line. The location of such earthquakes is therefore known and thus modeled by a point source. In contrast, subduction earthquakes of lower magnitudes are associated with partial rupture of the fault. The unknown location of this type of earthquakes is modeled by the line source shown in Figure 2.

In addition to the models required to simulate the earthquake hazard, an array of other models were utilized in this analysis. Table II provides an overview of these models. It is important to note that each model conforms to the following format: It takes random variables and other parameters as input, and it produces a physical measurable scalar or vector as output. For example, each of the earthquake location models described above takes the realization of a few random variables as input and produces the corresponding hypocenter location as output. Table II shows the number of instances of each model in the analysis. It also shows the number of random variables that each model takes. Specifically, the last two columns in Table II displays the number of aleatory random variables, size($\mathbf{x}$), and the number of epistemic random variables, size($\boldsymbol{\theta}$), respectively, in each model. It is emphasized that the models for building response and building damage, *i.e.*, the models in Table II that contain the word "Damage" or "Response" are simplified models rather than detailed finite element models. This is discussed later in the context of refining the building response and damage models.

3. Analysis

Given the sub-division of area sources in Figure 2 it is understood that there are 11 sources of earthquakes in the reliability analysis (Crustal + Subcrustal + Subduction = 6 + 3 + 2 = 11). As a result, a multi-hazard analysis is necessary. Several multi-hazard analysis options are available; one is the load coincidence method proposed by Wen (1990). However, matters simplify because the probability of coincidence of two earthquakes is negligible in this particular application. To address the presence of multiple hazards, let $i = \{1, 2, \ldots, N\}$, where $N = 11$ = number of hazards, and let β_i denote the reliability index associated with the limit-state function in Eq. (1) for each hazard. It is emphasized that each hazard is analyzed separately. From the theory of FORM reliability analysis it is know that the associated probability, *i.e.*, the point on the loss curve is

$$p_i = \Phi(-\beta_i) \tag{3}$$

where Φ is the standard normal cumulative distribution function. Provided the Poisson process is valid for each hazard, with rates λ_i, the rate of loss exceedance associated with each hazard is $\lambda_i p_i$. The combined rate including all hazards is the sum of the individual rates, and the Poisson distribution provides the probability of loss exceedance within a time period, T:

$$p = 1 - p(0) = 1 - \exp\left(-T \cdot \sum_{i=1}^{N} \lambda_i p_i\right) \tag{4}$$

In the context of FORM analysis is common to employ the reliability index instead of the probability. For this purpose, the generalized reliability index associated with p is obtained by inversion of the standard normal cumulative distribution function:

$$\beta = -\Phi^{-1}\left(p\right) \tag{5}$$

where β is employed in the following as a surrogate measure for the exceedance probability when all hazards are considered.

4. Loss Curve Results

As mentioned earlier, an important objective in this study is to compute loss curves. To illustrate the concept, Figure 3 shows two loss curves obtained by Monte Carlo sampling with 100,000 samples. The black solid line displays the loss curve that is obtained when all random variables are included. To highlight the significance of epistemic uncertainty, the grey line in Figure 3 shows the loss curve that is obtained if all the epistemic random variables, *i.e.*, $\boldsymbol{\theta}$, are set equal to their mean values. Naturally, this results in an underestimation of the probability of high losses, *i.e.*, a "slimmer" tail of the loss curve. In fact, particular focus in this study is on the tail of the loss curve because of its importance in risk mitigation decisions. Unfortunately, although Monte Carlo sampling is a robust analysis approach, it yields less accurate results in the tail than around the mean of the loss. In contrast, FORM has two advantages that are explored in this study. First, it is tailored to estimate small probabilities, *i.e.*, it addresses the tail of the loss curve. Second, it facilitates the computation of sensitivity measures that are employed in the following.

The loss curves in Figure 3 are plotted from zero to \$100 million, and the figure reveals that there is roughly a 5% chance that this loss threshold will be exceeded. A better estimate is obtained by running FORM analysis with the following limit-state function:

$$g = 100{,}000{,}000 - l\left(\boldsymbol{\theta}, \mathbf{x}\right) \tag{6}$$

FORM analysis for the individual hazards yield the reliability indices shown in Table III. The table shows that subduction earthquakes are associated with the lowest reliability indices. This implies that these earthquake sources produce the highest loss exceedance probabilities. However, it is also observed in Table III that subduction earthquakes are associated with low occurrence rates. This means that their overall influence on the seismic risk must be investigated further, which is done in the following. The results in Table III are substituted into Eq. (4) to compute the probability of exceeding a \$100 million loss considering all earthquake sources. This yields $p = 0.076$, *i.e.*, a 7.6% chance of exceeding that loss.

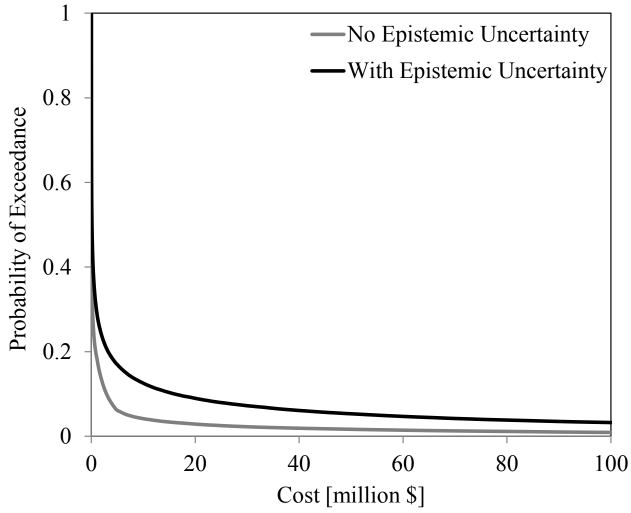

Figure 3. Loss curve with and without epistemic uncertainty.

TableIII: Occurrence rates and reliability indices for individual hazards.

Source	Occurrence Rate	Reliability Index
Crustal Area Source 1	0.062	3.5
Crustal Area Source 2	0.019	2.6
Crustal Area Source 3	0.017	2.5
Crustal Area Source 4	0.010	2.4
Crustal Area Source 5	0.017	2.6
Crustal Area Source 6	0.063	3.5
Subcrustal Area Source 1	0.0029	1.6
Subcrustal Area Source 2	0.027	2.0
Subcrustal Area Source 3	0.063	2.7
Subduction Line Source	0.0010	1.3
Subduction Point Source	0.0013	1.3

5. Sensitivity with respect to Model Refinement Decisions

In the context of the regional seismic risk analysis of the UBC campus, suppose it is contemplated to refine some of the building models to reduce the epistemic uncertainty. In particular, the analyst may seek to replace simple building response models with detailed finite element models. Clearly, only the most important buildings can be addressed due to the time it takes to establish a detailed finite element model and the added computational cost. This section provides guidance for the analyst to prioritize between buildings.

First, it is recognized that the objective is to reduce epistemic uncertainty. Provided that the epistemic uncertainty has been properly included in the models, a more detailed model will produce results with less uncertainty. Second, it is understood that it is the effect on the overall loss curve that must guide the decision to replace a model. In other words, the model whose $\boldsymbol{\theta}$ has the largest influence on p in Eq. (4) should be replaced with a better model. In particular, for a model with only one epistemic random variable, it is the sensitivity $\partial p/\partial\sigma$, where σ is the standard deviation of that epistemic random variable that should guide the prioritization. In general, each model has several epistemic random variables. To this end, a sensitivity measure that represents the derivative of p with respect to the standard deviation of all the epistemic random variables in a model is sought.

Suppose a model, such as the one in Eq. (2), is generically written as $y = y(\boldsymbol{\theta},\mathbf{x})$, where $\boldsymbol{\theta}$ and $\mathbf{x}$ remain the vectors of epistemic and aleatory random variables, respectively. Furthermore, let K denote the number of epistemic random variables in the model. Next, consider the well-known first-order approximation of the variance of the response from this model with respect to the epistemic random variables:

$$\sigma^2 = \nabla_{\boldsymbol{\theta}} y^T \cdot \boldsymbol{\Sigma}_{\boldsymbol{\theta\theta}} \cdot \nabla_{\boldsymbol{\theta}} y = \sum_{i=1}^{K}\sum_{j=1}^{K}\left(\frac{\partial y}{\partial \theta_i}\cdot\frac{\partial y}{\partial \theta_j}\cdot\rho_{ij}\cdot\sigma_i\cdot\sigma_j\right) \tag{7}$$

where $\nabla_{\boldsymbol{\theta}} y$ = gradient vector of y with respect to $\boldsymbol{\theta}$, $\boldsymbol{\Sigma}_{\boldsymbol{\theta\theta}}$ = covariance matrix of $\boldsymbol{\theta}$, ρ_{ij} = correlation coefficient between the components of $\boldsymbol{\theta}$, and σ_i = standard deviation of the components of $\boldsymbol{\theta}$. For models that are linear with respect to the epistemic random variables, Eq. (7) provides exact results; otherwise, it is an approximation. In order to study the influence of epistemic uncertainty on β, the following derivative is sought and evaluated by the chain rule of differentiation:

$$\frac{\partial\beta}{\partial\sigma} = \sum_{i=1}^{N}\left(\frac{\partial\beta}{\partial p}\cdot\frac{\partial p}{\partial p_i}\cdot\frac{\partial p_i}{\partial\beta_i}\cdot\frac{\partial\beta_i}{\partial\sigma}\right) \tag{8}$$

where N = number of hazards. The derivatives in the right hand side of Eq. (8) are addressed separately in the following. The first derivative is obtained by differentiating Eq. (5):

$$\frac{\partial\beta}{\partial p} = -\frac{1}{\varphi(\beta)} \tag{9}$$

The second derivative is obtained by differentiating Eq. (4):

$$\frac{\partial p}{\partial p_i} = T\cdot\lambda_i\cdot e^{-T\cdot\sum_{i=1}^{N}\lambda_i p_i} \tag{10}$$

The third derivative is obtained by differentiating Eq. (3):

$$\frac{\partial p_i}{\partial\beta_i} = -\varphi(\beta_i) \tag{11}$$

The fourth derivative is obtained by adding contributions from all the epistemic random variables in the model. The chain rule of differentiation yields:

$$\frac{\partial\beta_i}{\partial\sigma} = \sum_{j=1}^{K}\left(\frac{\partial\beta_i}{\partial\sigma_j}\cdot\frac{\partial\sigma_j}{\partial\sigma}\right) \tag{12}$$

where the first derivative in the right-hand side is a well-known reliability sensitivity measure, see for example Der Kiureghian (2005) for details, while the last derivative in the right-hand side of Eq. (12) is obtained by differentiating Eq. (7):

$$\frac{\partial \sigma}{\partial \sigma_j} = \frac{1}{\sigma} \cdot \frac{\partial y}{\partial \theta_j} \cdot \sum_{i=1}^{K} \left(\frac{\partial y}{\partial \theta_i} \cdot \rho_{ij} \cdot \sigma_i \right) \tag{13}$$

In the following, Eq. (8) is evaluated and compared for the 622 buildings at the UBC campus. Table IV displays values for $\partial\beta/\partial\sigma$ for the 10 highest ranked buildings. In other words, Table IV identifies the models for which a reduction in the epistemic uncertainty would have the greatest impact on the reliability index. Naturally, an increase in epistemic uncertainty, *i.e.*, an increase in σ, increases the probability of exceeding a \$100 million loss, which in turn reduces the reliability index; hence the minus sign in Table IV. It is observed in Table IV that the highest ranked buildings are mostly concrete shear wall buildings, which may indicate that the structural model for this type of building has the greatest potential for improvement. This point is brought up later in this paper.

Table V shows the ranking of magnitude models. It reveals that the magnitude model for subcrustal area source 2 is the model for which a reduction in the epistemic uncertainty would have the greatest impact on the loss probability. Similarly, Table VI shows the ranking of ground motion intensity models for an arbitrarily selected building. This ranking of the intensity models were observed for 430 of the buildings, while the intensity models for subduction and subcrustal earthquakes switch places for the other 192 buildings. It is reemphasized that these results provide a basis for selecting models to be refined if proper resources are available.

It is of interest to investigate the value of $\partial\beta/\partial\sigma$ if the entire collection of models is considered as one model. For this case, the evaluation of $\partial\beta/\partial\sigma$ is disaggregated into two parts:

$$\frac{\partial \beta}{\partial \sigma} = \sum_{i \in H} \frac{\partial \beta}{\partial \sigma_i} \cdot \frac{\partial \sigma_i}{\partial \sigma} + \sum_{i \in B} \frac{\partial \beta}{\partial \sigma_i} \cdot \frac{\partial \sigma_i}{\partial \sigma} \tag{14}$$

where the first sum is taken over epistemic random variables associated with hazard models, while the second sum is taken over epistemic random variables associated with building models. The analysis reveals that the first sum equals $-8.54 \cdot 10^{-9}$ and the second equals $-7.20 \cdot 10^{-7}$. This shows that, in the context of the epistemic uncertainty that is modeled in this study, it is far more effective to reduce the epistemic uncertainty in the building models rather than the hazard models.

6. Sensitivity with respect to Model Improvement Decisions

In the long run, researchers seek to improve the library of models that are available. This effort to reduce epistemic uncertainty in generic models addresses a different problem than that addressed in the previous section. In particular, the objective in the previous section was to identify, *e.g.*, the building that should be subjected to more detailed modeling. In contrast, this section identifies which generic models should be prioritized for further research and data gathering. To make such decisions, it is necessary to assess the cost of long-term model improvement, and how those efforts will improve the assessment of risk. To this end,

TableIV: Top 10 building models according epistemic uncertainty.

Building Name	Building Type	$\partial\beta/\partial\sigma$
University Centre Addition	Concrete Shear Wall	-0.76
Village Shops 2	Concrete Shear Wall	-0.57
Power House Meter Station	Concrete Shear Wall	-0.48
Vanier Pump Station	Steel Light Frame	-0.40
Wesbrook Animal Care Unit	Concrete Shear Wall	-0.27
St. Mark Chapel	Concrete Shear Wall	-0.11
Chan Centre for Performing Arts	Concrete Shear Wall	-0.11
Animal Science Main Sheep Unit	Concrete Moment Frame	-0.11
Morris & Helen Belkin Art Gallery	Concrete Shear Wall	-0.023
Village Shops 1	Concrete Shear Wall	-0.022

Table V: Ranking of magnitude models according to epistemic uncertainty.

Model	$\partial\beta/\partial\sigma$
Subcrustal Area Source 2 Magnitude	-0.097
Subcrustal Area Source 3 Magnitude	-0.062
Subcrustal Area Source 1 Magnitude	-0.023
Crustal Area Source 2 Magnitude	-0.019
Crustal Area Source 3 Magnitude	-0.019
Crustal Area Source 5 Magnitude	-0.018
Crustal Area Source 4 Magnitude	-0.017
Crustal Area Source 6 Magnitude	-0.0039
Crustal Area Source 1 Magnitude	-0.0034

Table VI: Ranking of intensity models according to epistemic uncertainty.

Model	$\partial\beta/\partial\sigma$
Crustal Intensity	-2.81
Subcrustal Intensity	-1.42
Subduction Intensity	-0.80

the sensitivity of the reliability index, β, with respect to the cost of modeling, c, *i.e.*, $\partial\beta/\partial c$, is sought. Chain rule of differentiation yields:

$$\frac{\partial \beta}{\partial c} = \sum_{i=1}^{N} \left(\frac{\partial \beta}{\partial \beta_i} \cdot \frac{\partial \beta_i}{\partial c} \right) \tag{15}$$

where the first derivative is expanded and explained earlier, and the second derivative is obtained by the chain rule, adding contributions over the K epistemic random variables of the model:

$$\frac{\partial \beta_i}{\partial c} = \sum_{j=1}^{K} \left(\frac{\partial \beta_i}{\partial \sigma_j} \cdot \frac{\partial \sigma_j}{\partial n} \cdot \frac{\partial n}{\partial c} \right) \tag{16}$$

where n is introduced to quantify the number of observations that are used to develop the model. The first derivative in the right-hand side of Eq. (16) is addressed in the previous section. The second derivative represents the change in the standard deviation of a model parameter due to a change in the number of observations that are employed to build the model. In the following, this derivative, $\partial\sigma_j/\partial n$, is expressed for three types of models: Linear regression models, nonlinear regression models, and generic models. For linear regression models, according to Box and Tiao (1992), the variance of the model parameter θ_j is

$$\sigma_j^2 = \frac{1}{n-k} \left(\mathbf{y} - \mathbf{X}\hat{\boldsymbol{\theta}} \right)^T \left(\mathbf{y} - \mathbf{X}\hat{\boldsymbol{\theta}} \right) \left(\left(\mathbf{X}^T \mathbf{X} \right)^{-1} \right)_{jj} \tag{17}$$

where k = number of θ-parameters in the model, $\mathbf{y}$ = vector of observed results, $\mathbf{X}$ = matrix of observations, $\hat{\boldsymbol{\theta}}$ = mean vector of model parameters, and $(\ )_{jj}$ identifies the j^{th} diagonal component. The variance of the model error is

$$\sigma_\varepsilon{}^2 = \frac{1}{n-k} \left(\mathbf{y} - \mathbf{X}\hat{\boldsymbol{\theta}} \right)^T \left(\mathbf{y} - \mathbf{X}\hat{\boldsymbol{\theta}} \right) \tag{18}$$

The derivative of Eq. (17) with respect to n is

$$\frac{\partial \sigma_j}{\partial n} = \frac{-\sigma_j}{2(n-k)} \tag{19}$$

and, similarly, the derivative with respect to Eq. (18) is:

$$\frac{\partial \sigma_\varepsilon}{\partial n} = \frac{-\sigma_\varepsilon}{2(n-k)} \tag{20}$$

Similar derivatives are obtained for nonlinear regression models, where the expressions analogous to Eqs. (17) and (18) are made available by Seber and Wild (2003). For generic models, such as finite element models, it is argued that the epistemic uncertainty is primarily present in the random variables that are input to the model. This is assumed here, although some efforts have been made by Haukaas and Gardoni (2011) and others to incorporate epistemic uncertainty into finite element models. To this end, it is of interest to identify how the epistemic uncertainty in a physical random variable say, concrete strength, is affected by inclusion of more information. As a starting point, consider the well-known expression for variance:

$$\sigma_j^2 = \frac{1}{n-1} \sum_{i=1}^{n} \left(x_i - \mu_j \right)^2 \tag{21}$$

where x_i = i^{th} observation and μ_j = mean of observations. The derivative is:

$$\frac{\partial \sigma_j}{\partial n} = \frac{-\sigma_j}{2(n-1)} \tag{22}$$

It is emphasized that the expressions for the derivative $\partial\sigma_j/\partial n$ are derived under the assumption that the mean model is unaffected by added observations. Clearly, this may not be the case in practical circumstances, where one added observation may precipitate an increase in the variance of the epistemic random variables. However, if the fundamental model form is correct, then over time, new data will serve to reduce the epistemic uncertainty. The previously presented formulas are derived on this basis.

It is observed that the minus sign in equations above for $\partial\sigma_j/\partial n$ correctly implies that that the standard deviation of the model parameter is reduced when n is increased. Moreover, it is observed that the reduction in the standard deviation is smaller when n is large than when n is small. In other words, a model that is based on a large number of observations will benefit less from a few more observations. Furthermore, it is observed that the reduction in the standard deviation is greater when k is large than when k is small. In other words, a model with more parameters, *i.e.*, a more complex model, will benefit more from new observations.

The last derivative in the right-hand side of Eq. (16) is the inverse of the cost of obtaining one data point. Naturally, the quantification of this cost is challenging. In fact, some observations are readily obtained, while others come at a significant cost. Examples of typical engineering observations that are counted by n include: 1) Testing of building on a shake table, which can be used to calibrate the building response, damage, and repair cost models; 2) Analysis of a highly refined numerical building model, which can be used to calibrate building response models; 3) Survey of buildings damaged in earthquakes, which can be used to calibrate building damage models; and 4) Claims reports from insurance companies, which can be used to calibrate building damage models. Although the cost of obtaining such data vary, it is assumed in this study that each observation will take two to three days of paid work and cost around $500, *i.e.*, $\partial c/\partial n = 500$.

The sensitivity measure $\partial\beta/\partial c$ is now evaluated for the models that were employed in the regional risk analysis for the 622 buildings at the UBC campus. The model types were presented in Table II. Table VII identifies the five models with highest value of $\partial\beta/\partial c$. This means that allocating resources for improving these models has the greatest impact on the reliability index. In particular, gathering data to improve the concrete shear wall structural response model has the greatest effect on the reliability index per dollar spent.

The positive sign of the $\partial\beta/\partial c$-values indicates that the reliability index increases when resources are allocated to data gathering. This makes sense, because the resulting model improvement reduces the uncertainty, which in turn reduces the probability of exceeding a $100 million loss. This decrease in probability is reflected by the increase in the reliability index, which is correctly captured by the positive sign of the $\partial\beta/\partial c$-values.

Table VIII identifies the five models with lowest value of $\partial\beta/\partial c$. In other words, these are the models for which data gathering and model improvement would not have significant impact on the reliability index. While structural response models rank highest according to $\partial\beta/\partial c$, structural damage models rank lowest. In other words, in the context of the models employed in this study, it appears worthwhile to focus attention on reducing the epistemic uncertainty in the structural response models, *i.e.*, models for building displacement and acceleration, rather than the damage models. However, an important remark is made in regards to these results: The ranking according to $\partial\beta/\partial c$ depends on the number of instances of a model type in the analysis. For example, in the present analysis, almost 54% of the building value is associated with concrete shear wall buildings, *i.e.*, buildings of the type that ranked first in Table VII. On one hand, this skews the results towards higher $\partial\beta/\partial c$-values for this building type. Although this is not the only reason for the observed result, it should be duly noted when applying these results to regions with other compositions of the building stock. On the other hand, the ranking in Table VII and Table VIII are still valuable for the considered region. For researchers who seek to improve the risk assessment for this particular region, the results in Table VII and Table VIII are valid as measures to guide the allocation of resources for model improvement.

An additional remark about the results in Table VII, particularly the high rank of concrete shear wall structural response models, is made in regards to the results in the previous section. There it was noted that several of the concrete shear wall buildings are primary candidates for more refined structural analysis to reduce epistemic uncertainty. It is interesting to note that this type of building consistently ranks high according to both sensitivity measures.

Table VII: Top five model types according to cost of model improvement.

Model Type	$\partial\beta/\partial c$ [$\cdot 10^{-6}$]
Concrete Shear Wall Structural Response	46.7
Wood Large Frame Structural Response	4.4
Wood Light Frame Structural Response	1.0
Concrete Frame with Masonry Infill Wall Structural Response	0.52
Concrete Moment Frame Structural Response	0.50

Table VIII: Bottom five model types according to cost of model improvement.

Model Type	$\partial\beta/\partial c$ [$\cdot 10^{-12}$]
Wood Light Frame Structural Damage	0.2
Steel Light Frame Structural Damage	0.09
Steel Braced Frame Structural Damage	0.06
Steel Moment Frame Structural Damage	0.03
Steel Frame with Masonry Infill Wall Structural Damage	0.02

7. Conclusions

The overarching vision behind this paper is twofold. First, it is sought to identify and characterize epistemic uncertainty in a comprehensive manner. This is important because epistemic uncertainty, such as model uncertainty, is reducible and has significant influence on risk estimates. Second, it is sought to allocate resources in an optimal manner to reduce the epistemic uncertainty. The first goal is achieved by utilizing a library of probabilistic models that contain random variables that represent epistemic uncertainty. These models are implemented in a computer program, called Rt, dedicated to multi-model reliability analysis. Rt is employed in this paper to conduct risk analysis for a region in Vancouver, Canada that comprises 622 buildings. The second goal is addressed in this paper by the development of two new reliability sensitivity measures. These are implemented in Rt and evaluated in the regional risk analysis. The results show that the epistemic uncertainty associated with the models for concrete shear wall buildings is the most cost-effective to address for this region.

Acknowledgements

The financial support from the Natural Science and Engineering Research Council of Canada (NSERC) through the Strategic Project Grant number 336498-06 is gratefully acknowledged. The first author also thanks the Killam Trusts for support in the form of a Killam Doctoral Fellowship. The authors also thank Mr. Aprizal Kristijanto for surveying buildings at the campus of the University of British Columbia in Vancouver.

References

Box, G. E. P., and G. C. Tiao. *Bayesian inference in statistical analysis*. New Jersey: Wiley-Interscience, 1992.

Der Kiureghian, A. First-and second-order reliability methods. In *Engineering design reliability handbook.*, eds. E. Nikolaidis, D. M. Ghiocel and S. Singhal. Boca Raton, FL: CRC Press, 2005.

Gardoni, P., A. Der Kiureghian, and K. M. Mosalam. Probabilistic capacity models and fragility estimates for reinforced concrete columns based on experimental observations. *Journal of Engineering Mechanics* 128 (10): 1024-38, 2002.

Mahsuli, M., and T. Haukaas. A computer program for multi-model reliability and optimization analysis. *Journal of Computing in Civil Engineering,* In Press, 2012.

Seber, G. A. F., and C. J. Wild. *Nonlinear regression*. New York: Wiley-IEEE, 2003.

Wen, Y. K. *Structural load modeling and combination for performance and safety evaluation*. Amsterdam, Netherlands: Elsevier, 1990.